ELSEVIER

Surface Science 505 (2002) 349–357

SURFACE SCIENCE

www.elsevier.com/locate/susc

# Effect of mass and incidence angle of keV energy polyatomic projectiles in silicon sputtering

M. Medvedeva, I. Wojciechowski, B.J. Garrison *

*Department of Chemistry, 152 Davey Laboratory, Pennsylvania State University, University Park, PA 16802-6300, USA*

Received 27 September 2001; accepted for publication 23 January 2002

**Abstract**

Recent experiments of bombardment of silicon targets show that keV energy polyatomic projectiles can greatly increase both the total yield and the secondary silicon ion emission, especially complex secondary ions. This effect is more pronounced for the heavy polyatomic projectiles than for light ones. To understand why the heavy projectiles increase the non-linear enhancement of the yields, molecular dynamics simulations of the bombardment of a Si(1 0 0)–$(2 \times 1)$ surface by $Al_n$ ($n = 1, 2$) and $Au_n$ ($n = 1, 2$) projectiles with $E_0 = 1.5$ keV/atom at the incident angles of $\theta = 0°$ and $\theta = 45°$ have been carried out. It is shown that oblique bombardment by heavy dimer projectiles at this initial energy leads to an increase of the number of trajectories with a very high yield of ejected atoms. A microscopic analysis of the events is given and also the influence of the high yield events on the energy distributions of the sputtered silicon atoms is described. 

*Keywords:* Computer simulations; Sputtering; Energy dissipation; Silicon

## 1. Introduction

The use of polyatomic projectiles has the potential to create the optimal conditions required for secondary ion mass spectrometry (SIMS) analysis of large organic species, including biomolecules and synthetic polymers adsorbed on different surfaces, as well as to offer some advantages for depth profiling of both ultrashallow dopant profiles and metals [1–9]. The specific question, which is still open in analytical studies, is how to optimize the different primary beam parameters, e.g. primary particle mass, energy, incident angle, and the number of projectile constituents for a given target to obtain the desired improvement of the sensitivity of SIMS.

One of the fascinating observations in experiments with polyatomic bombardment is that polyatomic projectiles can greatly increase both the total yield and the secondary ion emission with respect to atomic projectiles [10]. This effect is more pronounced for complex secondary ions [11–13]. The apparent enhanced yield could, in fact, be merely due to the fact that there are more projectiles. In order to remove the effect of numerous incident particles, an enhancement factor is defined. When the emission yield induced by polyatomic projectile containing $n$ atoms is larger than $n$ times the yield for one atom at the same velocity per atom, then

* Corresponding author. Tel.: +1-814-863-2103; fax: +1-814-863-5319.

*E-mail address:* bjg@chem.psu.edu (B.J. Garrison).

0039-6028/02/$ - see front matter 
PII: S0039-6028(02)01387-0

there is "non-linear enhancement" of the yield. Specifically for polyatomic projectiles, the enhancement factor is

$$k_{n,m} = \frac{mY_n}{nY_m}, \quad (1)$$

where $Y_n$ and $Y_m$ are the emission yields induced at identical impact velocities by projectiles having $n$ and $m$ constituents, correspondingly. If $k_{n,m} > 1$ for $n > m$, then the ratio in Eq. (1) reflects the amount of non-linear enhancement of the emission yield under polyatomic impact.

A strong non-linear enhancement in the total sputtering yield of gold atoms was observed for $Au_n^+$ ($n = 1$–5) projectile impact of a gold metallic target [14] at energies 20–5000 keV/atom. For example, the impact of a single $Au_5^+$ cluster was reported to produce on average 3000 secondary gold atoms, while a single $Au^+$ projectile ejects only 55 atoms at the initial energy of 150 keV/atom. Bombardment by $Au_2$ is particularly interesting because they can be made in liquid metal ion guns and used for surface imaging experiments [15,16]. Many of the applications for the imaging experiments involve usage of biological and organic solids in which the atomic mass of the target is considerably less than the polyatomic projectile atoms.

The sputtering from a polycrystalline silicon target induced by $Au_n^-$ ($n = 1$–3) and $Al_n^-$ ($n = 1$, 2) ions with the initial energies from 6 to 18 keV/atom was recently investigated in [12,13]. The polyatomic gold ion bombardment was found to increase the contribution of large clusters of $Si_n^+$ ($n \geqslant 4$) to the total yield of charged particles. In the case of $Au^-$ and $Au_2^-$ bombardment at a primary energy of 9 keV/atom, the $k_{2,1}$ for $Si_4^+$ and $Si_6^+$ are 40 and 200, respectively. The cluster contribution to the total yield increases with increasing incident energy. The projectiles $Al^-$ and $Al_2^-$ are less effective at producing large cluster ion emission. An increase of the large secondary cluster yield is obtained by decreasing the incident energy of the $Al_2^-$ projectiles. This observation indicates that the non-linear enhancement of the sputtering yield has a complex behavior vs. incident energy and incident particle type.

The molecular dynamics (MD) computer simulation approach has been quite successful in modeling the polyatomic bombardment of metal substrates [17–20] and organic overlayers on metal and silicon substrates [21–25]. These works have confirmed that the surface structure and the number of atoms in the projectile affect the character of the events developed within the crystal after the projectile impact. The openness of the Si substrate is more effective for intact organic molecule desorption compared to the close-packed metal substrate under low energy polyatomic projectile bombardment [23,24]. The polyatomic projectiles consisting of lighter mass atoms lead to a greater yield of ejected molecules than atomic projectiles of heavier mass.

The purpose of the present simulations is to understand how heavy Au polyatomic projectiles relative to the lighter Al projectiles can create the conditions favorable for high yield events inducing the non-linear enhancement of both the total and cluster yield for Si substrate. The MD simulations of the interaction of $Al_n$ and $Au_n$ ($n = 1$, 2) projectiles at the same initial energy per atom with the silicon surface are performed. We use different incidence angles to demonstrate the influence of this parameter on emission of Si clusters. Comparing Al and Au bombardment, the $Au_2$ projectile at oblique incidence is better for high yield events, thus enhancing both the total and cluster yields.

## 2. Method

MD simulations have been carried out to model the interaction of $Al_n$ and $Au_n$ ($n = 1$, 2) with a Si(1 0 0)–(2 × 1) surface. The projectiles hit the substrate with an initial energy $E_0 = 1.5$ keV/atom at incident angles of $\theta = 0°$ and $\theta = 45°$.

The classical MD simulations have been described extensively elsewhere [26,27]. Briefly, the method consists of numerically integrating Hamilton equations of motion to determine the position and the velocity of each particle as a function of time. Pair and many-body interaction potentials describe the energies and forces in the system. Experimentally observable properties are calcu-

lated from the final positions, velocities and masses of the ejected species. Mechanistic information is obtained by monitoring the time evolution of relevant collision events.

The dimer reconstructed Si(1 0 0)–(2 × 1) microcrystallite consisting of about 9000 atoms with 10 layers is used. The orientation of the dimer projectiles with respect to the surface is selected randomly. To obtain average yields, 1950 trajectories are calculated for each combination of projectiles and incident angle. The integration of any run is terminated either when no particle within the target volume has sufficient energy to eject, or when a cutoff time of 3 ps is reached. Because the action in the substrate is much larger in the case of $Au_2$ bombardment at $\theta = 45°$ than for the other systems, the average yields in this case are calculated with 150 trajectories with a cutoff time of 8 ps. The microscopic analysis is performed with 150 trajectories.

Open boundary conditions are used for the system [26]. That is, energetic particles that reach the sides or bottom of the microcrystallite are allowed to exit, taking their energy with them. Ultimately, these atoms will penetrate into extended regions of the crystal.

The forces among the atoms are described by the best available empirical potential energy functions. The MD-MC/CEM potential developed by DePristo and coworkers [28–30] is used for the Al–Al and Au–Au interactions. The Tersoff potential is used for Si–Si interaction [31]. A purely repulsive Molière potential is used to describe the interactions between the Al–Si and Au–Si atoms.

At the end of each simulation, the atoms and clusters, which have velocities directed towards the vacuum and are at distances of more than 6 Å above the original sample, are regarded as ejected. For identifying clusters, pairs of atoms are checked to see if there is an attractive interaction between them, in which case they are considered as linked [27]. A network of linked pairs is constructed and the total internal energy of the group is evaluated. If the total internal energy is less than zero, then the group of atoms is considered as an ejected cluster. The process of cluster dissociation before reaching the detector [32] is not considered in our simulations for two reasons. First, the short time fragmentation changes fractions of sputtered clusters containing different number of atoms, but does not dramatically decrease the total cluster yield. Furthermore, the Si–Si potential [31], which realistically describes the silicon binding in the crystal, is not expected to describe adequately the binding of Si clusters in the vacuum.

## 3. Results and discussion

The total and cluster yields as well as their enhancement factors have been calculated vs. the atom mass of projectile constituents, the number of atoms in the projectile and the incident angle. The results obtained are explained in terms of the specific mechanism of the interaction of the projectiles with the substrate atoms. The results show a pronounced enhancement of both the total yield and the cluster yield for $Au_2$ bombardment at 45° angle of incidence.

### 3.1. Enhancement of the total and the cluster yields

The average total and cluster sputtering yields are given in Table 1 for Al, $Al_2$, Au and $Au_2$ bombardment of the Si(1 0 0)–(2 × 1) surface along the surface normal and at the angle of incidence of 45° for the energy of 1.5 keV/atom. The average yields are calculated as the raw number of all sputtered Si atoms for the total yield and the raw number of Si atoms linked in clusters for the cluster yield divided by the total number of trajectories. The enhancement factor is calculated by

$$k_{2,1} = Y_2/2Y_1, \tag{2}$$

where $Y_1$, $Y_2$ are the yields induced by atomic and dimer bombardment at the same impact velocities, respectively. The cluster fraction is calculated as a ratio of the number of atoms comprising the sputtered clusters to the total number of sputtered Si atoms.

It is seen in Table 1 that $k_{2,1} > 1$ for all cases when going from atomic to dimer bombardment. The enhancement factors reported in Table 1 of slightly larger than 1 are typical of values other investigators have reported for metallic [20] and organic overlayers on metal and silicon substrates

Table 1
The average yields and the enhancement factors for Al, $Al_2$, Au and $Au_2$ bombardment with $E_0 = 1.5$ keV/atom at $\theta = 0°$ and $\theta = 45°$[a]

| Angle | Projectile | Total yield | $k_{2,1}$-total yield | Cluster yield | $k_{2,1}$-cluster yield | Cluster fraction |
|---|---|---|---|---|---|---|
| 0° | Al | 1.2 | | 0.4 | | 0.3 |
| | $Al_2$ | 3.3 | 1.4 | 1.7 | 2.1 | 0.52 |
| | Au | 1.2 | | 0.4 | | 0.3 |
| | $Au_2$ | 4.2 | 1.7 | 2.1 | 2.6 | 0.64 |
| 45° | Al | 3.0 | | 1.1 | | 0.37 |
| | $Al_2$ | 10.0 | 1.7 | 6.3 | 2.9 | 0.63 |
| | Au | 5.3 | | 3.2 | | 0.60 |
| | $Au_2$[b] | 74.0 | 7.0 | 69.3 | 10.8 | 0.94 |

[a] A total of 1950 trajectories were calculated for each set of initial conditions with a maximum time of 3 ps unless noted otherwise.
[b] A total of 150 trajectories with a maximum time of 8 ps are calculated.

[24]. The enhancement factor of 7 for $Au_2$ vs. Au bombardment at 45°, however, is larger than heretofore reported in simulations. Moreover, the computational approximations of a finite microcrystallite size and finite simulation time will tend to make the calculated $Au_2$ yield at 45° too small, thus, the real enhancement could be even larger. The dimer bombardment enhances the cluster yield relative to the total (and monomer) yield, an observation also found for metal substrates [20].

The different character of the $Au_2$ bombardment at 45° is shown in Fig. 1(a) and (b) where we have plotted the probability distributions of trajectories leading to the simultaneous emission of a given number of particles. We have grouped the number of ejected Si atoms per incident particle into groups of 10. The number of trajectories leading to the emission of a number of atoms belonging to a given bin are summed and divided by the total number of trajectories. The trajectories having no ejected atoms are considered in the first bin. The trajectories sputtering more than 150 atoms are taken into account in the last bin. In general, most of the primary projectiles eject less than 10 atoms in a single impact event. The exception is $Au_2$ bombardment at $\theta = 45°$ where as many as 200 atoms can eject in one impact.

The ramifications of the probability distributions shown in Fig. 1(a) and (b) on the total yield of sputtered particles are given in Fig. 1(c) and (d). In the case of $Au_2$ bombardment at $\theta = 45°$, the yield increase is mainly caused by the trajectories in which more than 40 atoms are ejected. Trajectories that give rise to a large number of sputtered atoms are, of course, the ones that are most probable for cluster formation. The mechanistic reasons for the large yields with $Au_2$ bombardment are given below.

### 3.2. Microscopic view of the dimer interaction with the silicon surface

The process of energy transfer from the projectile to the surface depends on the mass ratio of the incoming and substrate atoms as well as the projectile initial velocity and the substrate structure. The difference between the masses of the Al (27 amu) and Au (197 amu) atoms is large. As a result, the character of collision event development after penetration of these particles into the silicon (28 amu) substrate is quite different. Although the yields are representative of the final positions of the particles, we have found that the essential physics leading to this large enhancement is apparent at 28 fs into the trajectory. This time is convenient for analysis because almost all the incident particles are still in the microcrystallite used in the simulations.

It has been established in Ref. [22] that production of high yield events and, as a consequence, the enhanced sputtering yield, are unambiguously connected with the amount of energy deposited in the substrate and the degree of the energy localization with respect to the depth and the bulk. An overview of the trajectories at 28 fs is shown in Fig. 2 for 45° incidence, where the positions of Al

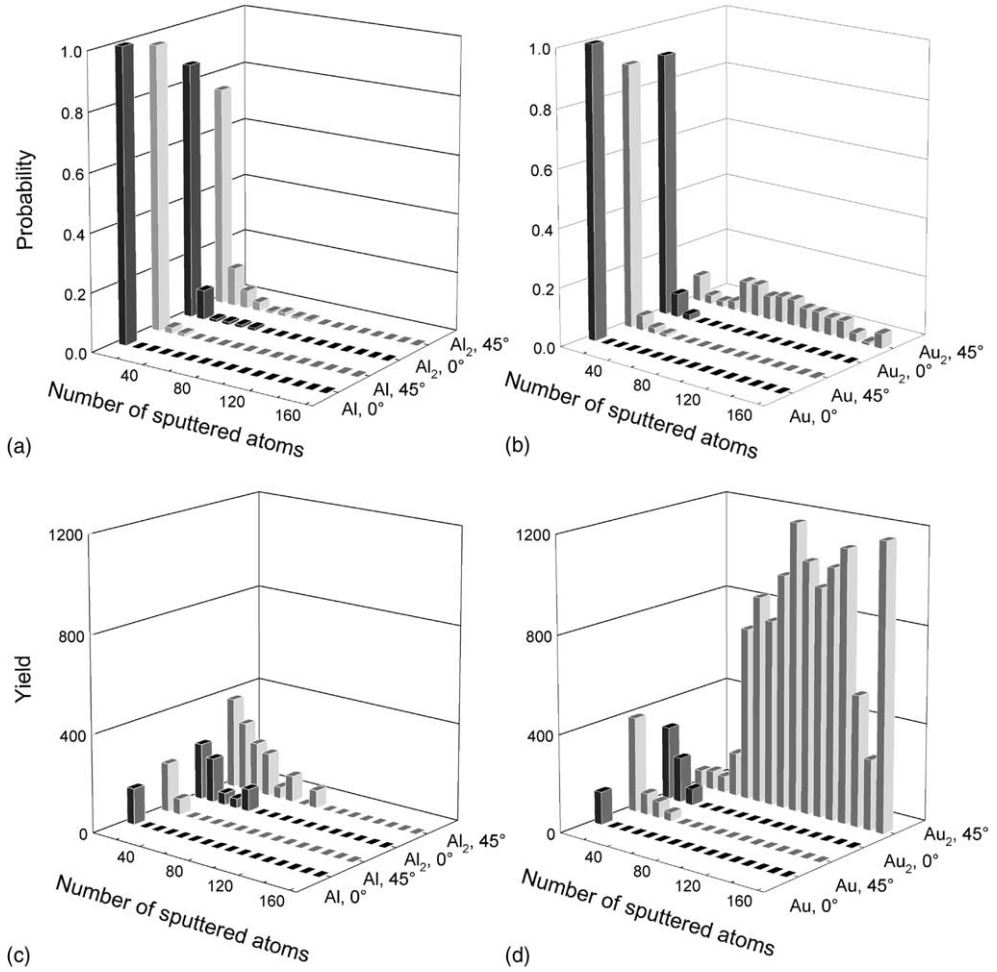


Fig. 1. Probability distributions and associated yield distributions over the number of sputtered Si atoms for aluminium (a, c) and gold (b, d) projectiles at the normal and 45° incident angle.

and Au projectile atoms are graphically displayed. The Al atoms are spread over the crystal bulk in the first 28 fs, whereas most of the Au atoms are localized in a small region near the surface. Not only are the Au atoms remaining closer to the surface but the average energy deposited per slab of 1 Å depth of the Si microcrystallite is more for the gold projectiles than the aluminum ones as shown in Fig. 3. There are several interrelated effects transpiring simultaneously.

- Al is lighter and smaller than Au, thus at these kinetic energies it can travel larger distances in the Si substrate than the Au atoms (Fig. 2). Consequently, its energy is deposited over a greater depth (Fig. 3).
- The nearly identical masses of Al and Si allow almost complete energy transfer in a single collision. Numerous Si atoms have also moved large distances in the first 28 fs thus taking energy away from the near surface region. In contrast, the Au atoms give up small amounts of energy to many Si atoms.
- The maximum scattering angle for an Au atom hitting a Si atom is only 8°. The Au atoms do not diverge much from their original path as

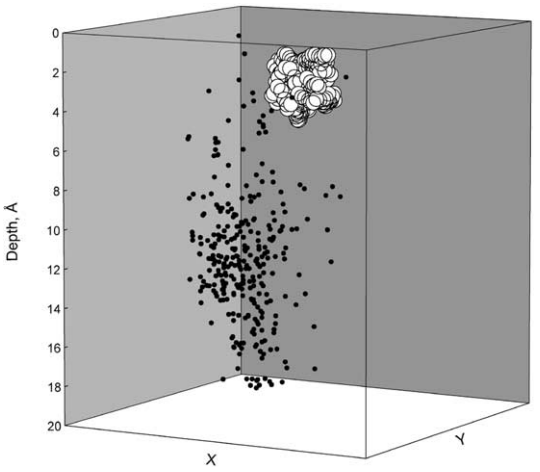


Fig. 2. Bulk distribution of the Al (the small dark spheres) and Au (the large light spheres) atoms at 28 fs. These are 150 dimer projectile impacts at $\theta = 45°$.

clearly shown in Fig. 2. Moreover, the two Au atoms remain together as dimer through the first 28 fs.

The concept that the Au atoms maintain their identity as a dimer is shown more clearly in Fig. 4 where the probability for the $Al_2$ and $Au_2$ constituents to be at a given distance, expressed in units of the equilibrium internuclear distance for each dimer $r_0$, is shown for time intervals of 28 and 50 fs. It is seen that upon penetrating into the substrate the $Al_2$ constituents quickly disintegrate in the initial part of the trajectory, acting independently thereafter. In contrast, the $Au_2$ constituents act together for a longer time. Cascades created by gold dimer constituents overlap with a large probability, and many Si atoms are displaced in a small region. As a result, the deposited energy is localized within a relatively small narrow surface region, where all atoms are set in motion. In this case, more damage is created and it is harder for either Au or Si atoms to penetrate into channels and escape from the collision region.

The one particle nature of the $Au_2$ molecule is reinforced in Fig. 5 where the remaining energy of the Au atoms is given at 28 and 50 fs. It is seen that the Au atoms that are part of a dimer penetrate

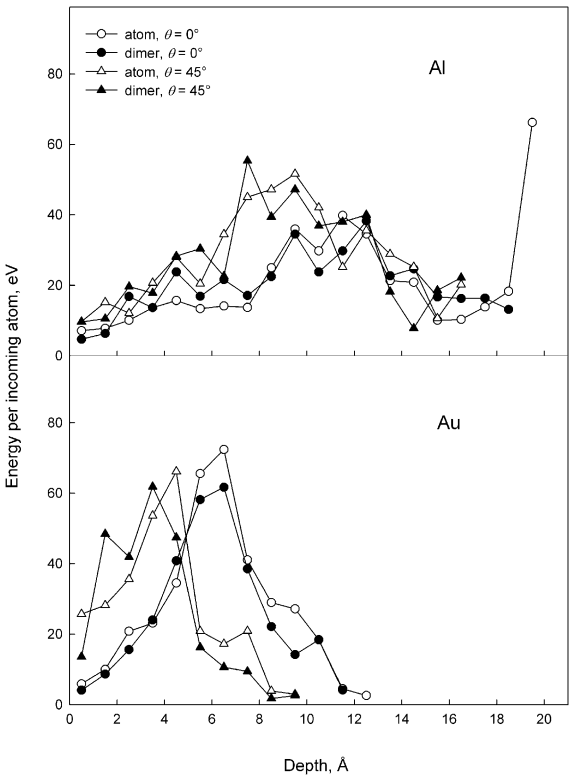


Fig. 3. Distributions of the average energy deposited by one incoming atom over the crystal depth at 28 fs after the impact for all the bombardment systems. The silicon microcrystallite is divided into slabs of 1 Å depth. The kinetic energies of the silicon atoms in a given slab after 28 fs are summed over all the trajectories and are then divided by the number of all the incoming atoms. If the Si atom coordinate is more than 19 Å, then it is considered as penetrating deeper into the crystal.

less deeply into the bulk than the atomic projectiles. The dimer constituents deposit their energy more slowly than the atomic projectiles. For dimer bombardment, more atoms keep their initial energy after 50 fs. The process of sharing and depositing energy is slow and more effective in the $Au_2$ case, thus increasing the probability of high yield events for enhancement of both the total and cluster yields.

The angle of incidence dependence is illustrated in Fig. 3. The $Au_2$ dimers aimed normal to the surface deposit their energy more deeply ($\sim$5–8 Å) into the substrate than those aimed at 45°. This distance is too deep for effective sputtering.

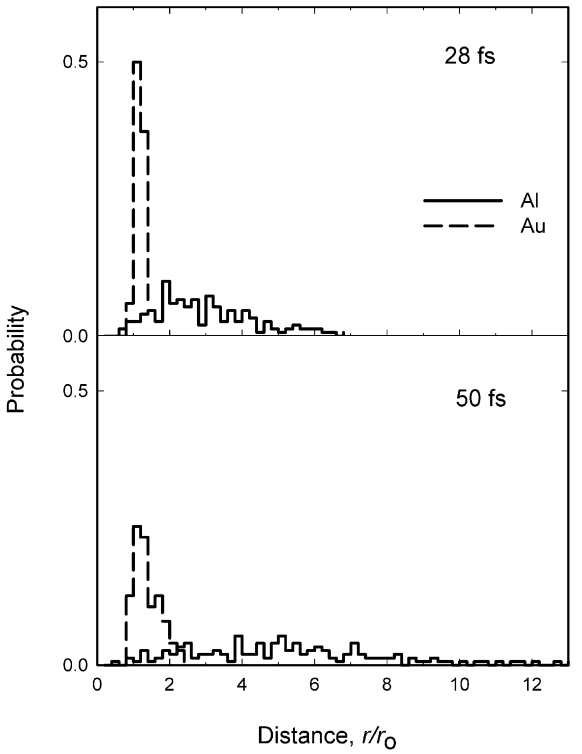


Fig. 4. Probability distributions of the distance between dimer constituents at 28 and 50 fs after the impact. The distance is expressed in units of the equilibrium internuclear distance $r_0$ for each type of projectile. The values of $r_0$ for $Al_2$ and $Au_2$ are 2.67 and 2.47 Å, respectively.

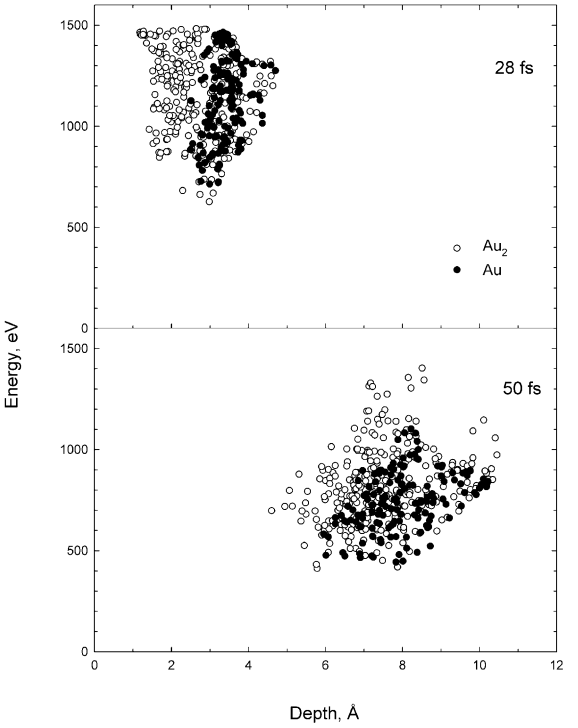


Fig. 5. Scatter plot distributions of the Au atom energy over the crystal depth at 28 and 50 fs after the impact, obtained for 150 trajectories at $\theta = 45°$ with $Au_2$ and Au projectiles.

### 3.3. Kinetic energy distributions of the sputtered silicon monomers

In addition to increasing yields, cluster fractions and enhancement factors, it has been shown in Ref. [22] that high yield events can affect the kinetic energy distributions (KEDs) of intact organic molecules sputtered from the metal surfaces. To check the influence of high yield events on the KEDs of sputtered Si atoms, angle-integrated KEDs of silicon monomers sputtered by Au and $Au_2$ projectiles at $\theta = 0°$ and $\theta = 45°$ are calculated and shown in Fig. 6. The form of the distribution for Au projectiles at normal incidence is typical for atomic sputtering [33]. For both Au and $Au_2$ projectiles at $\theta = 45°$, the KEDs are broader with increased low (<1 eV) and high energy contributions. The increase at high kinetic

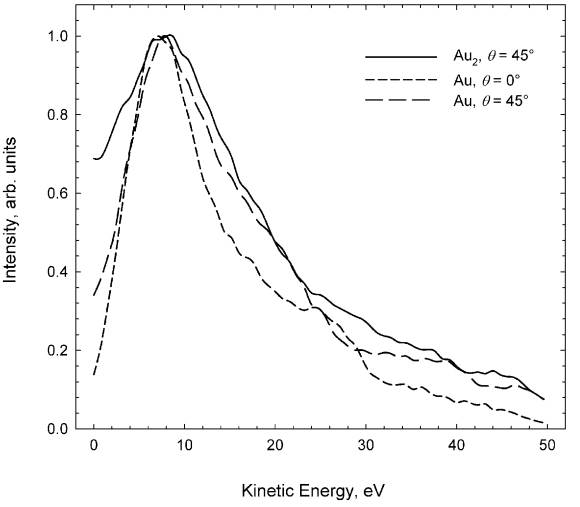


Fig. 6. Angle-integrated KEDs of ejected Si monomers for Au and $Au_2$ bombardment with $E_0 = 1.5$ keV/atom at $\theta = 0°$ and $\theta = 45°$. All the distributions are peak normalized to unity.

energy is explained by the concentration of the collision cascades in the near surface region [34,35]. The appearance of the low energy monomers is connected with the large number of low energy Si atoms ejected in the large damaged region. As mentioned in the previous section, the probability of creation of this region is greater for $Au_2$. Moreover, it is created nearer to the surface. As a consequence, the number of low energy sputtered Si monomers is the largest in this case.

## 4. Conclusion

MD calculations have been performed on a Si(1 0 0)–(2 × 1) surface with $Al_n$ and $Au_n$ ($n = 1$, 2) projectiles at the initial energy of 1.5 keV/atom for incident angles of $\theta = 0°$ and $\theta = 45°$. The non-linear enhancements in the total and cluster yields have been determined under dimer bombardment for each projectile/silicon surface system at both incident angles. Both the total and cluster yields of sputtered silicon species are greater at $\theta = 45°$ than those at $\theta = 0°$ for all the projectiles. The largest enhancement factor for the total and cluster yields is predicted for $Au_2$ at $\theta = 45°$ bombardment. The microscopic analysis of interaction of atomic and dimer projectiles at $\theta = 0°$ and $\theta = 45°$ displays that differences between Au and Al projectiles become pronounced even at the beginning of the trajectory evolution, i.e., at 28 fs after impact.

The bombardment at $\theta = 45°$ creates a high energy density region close to the surface. Heavy gold atoms have less initial velocity than light aluminum ones at the same $E_0$ and stay near the surface for longer time. The collisions of Au and Si atoms produce less energetic recoils than Al–Si collisions. As a result, the process of transferring energy to the substrate for Au occurs more slowly than for Al. The gold dimer constituents stay in the vicinity of each other for a much longer time than the constituents of an aluminum dimer, thus increasing the density of deposited energy in the subsurface region. Consequently, there are many high yield events, which, in turn, lead to the increase of the cluster particle sputtering.

Our simulations show that the gold dimer with the initial energy of 1.5 keV/atom at $\theta = 45°$ enhances the cluster yield of Si significantly. These results are qualitatively consistent with the recent experimental data, where the large non-linear enhancements of both the total yield and the cluster one under $Au_2$ projectiles at the same incident angle has been established.

## Acknowledgements

The financial support of the National Science Foundation through the Chemistry Division and the MRI program is gratefully acknowledged. Additional computational resources were provided in part by the IBM Selected University Resource Program and the Center of Academic Computing of Penn State University. The authors thank Kristin Krantzman and Arnaud Delcorte for helpful discussions and advice. M.M. thanks the PCPM laboratory (Université Catholique de Louvain) for providing computer facilities.

## References

[1] P.A. Ronsheim, G. Fitzgibbon, J. Vac. Sci. Technol. B 10 (1992) 329.
[2] H. Yamazaki, Y. Mitani, Nucl. Instrum. Meth. B 124 (1997) 91.
[3] G. Gillen, M. Walker, Ph. Thompson, J. Bennett, J. Vac. Sci. Technol. B 18 (2000) 503.
[4] G. Gillen, S. Roberson, Rapid Commun. Mass Spectrom. 12 (1998) 1303.
[5] G.S. Groenewold, J.E. Delmore, J.E. Olson, A.D. Appelhance, J.C. Ingram, D.A. Dahl, Int. J. Mass Spectrom. Ion Process. 163 (1997) 185.
[6] G.S. Groenewold, A.K. Gianotto, J.E. Olson, A.D. Appelhans, J.C. Ingram, J.E. Delmore, A.D. Shaw, Int. J. Mass Spectrom. Ion Process. 174 (1998) 129.
[7] F. Kötter, A. Benninghoven, Appl. Surf. Sci. 133 (1998) 47.
[8] D. Stapel, O. Brox, A. Benninghoven, Appl. Surf. Sci. 140 (1999) 156.
[9] E.R. Fuoco, G. Gillen, M.B.J. Wijesundara, W.E. Wallace, L. Hanley, J. Phys. Chem. B 105 (2001) 3950.
[10] Y. Le Beyec, Int. J. Mass Spectrom. Ion Process. 174 (1998) 101.
[11] M.J. Van Stipdonk, R.D. Harris, E.A. Schweikert, Rapid Commun. Mass Spectrom. 11 (1997) 1794.
[12] S.F. Belykh, A.P. Kovarsky, V.V. Palitsin, A. Adriaens, F. Adams, in: Abstracts of 19th International Conference on Atomic Collision in Solids (ICACS-19), Paris, France, 2001, p. 220.
[13] S.F. Belykh, A.P. Kovarsky, V.V. Palitsin, A. Adriaens, F. Adams, Int. J. Mass Spectrom. 209 (2001) 141.

[14] H.H. Andersen, A. Brunelle, S. Della-Negra, J. Depauw, D. Jacquet, Y. Le Beyec, J. Chaumont, H. Bernas, Phys. Rev. Lett. 80 (1998) 5433.
[15] B. Hagenhoff, R. Kersting, D. Rading, S. Kayser, E. Niehuis, in: A. Benninghoven, P. Bertrand, H.-N. Migeon, H.W. Werner (Eds.), Secondary Ion Mass Spectrometry SIMS XII, Elsevier, 2000, p. 833.
[16] A.V. Walker, N. Winograd, Appl. Surf. Sci., in press.
[17] M.H. Shapiro, T.A. Tombrello, Nucl. Instrum. Meth. B 152 (1999) 221.
[18] T.J Colla, H.M. Urbassek, Nucl. Instrum. Meth. B 164–165 (2000) 687.
[19] T.J Colla, R. Aderjan, R. Kissel, H.M. Urbassek, Phys. Rev. B 62 (2000) 8487.
[20] M. Lindenblatt, R. Heinrich, A. Wucher, B.J. Garrison, J. Chem. Phys. 115 (2001) 8643.
[21] B.J. Garrison, in: J.C. Vickerman, D. Briggs (Eds.), ToF-SIMS: Surface Analysis by Mass Spectrometry, IM Publications and SurfaceSpectra Limited, 2001, p. 223.
[22] A. Delcorte, B.J. Garrison, J. Phys. Chem. B 104 (2000) 6785.
[23] J.A. Townes, A.K. White, E.N. Wiggins, K.D. Krantzman, B.J. Garrison, N. Winograd, J. Phys. Chem. A 103 (1999) 4587.
[24] T.C. Nguyen, D.W. Ward, J.A. Townes, A.K. White, K.D. Krantzman, B.J. Garrison, J. Phys. Chem. B 104 (2000) 8221.
[25] B.J. Garrison, A. Delcorte, K.D. Krantzman, Acc. Chem. Res. 33 (2000) 69.
[26] D.E. Harrison Jr., Crit. Rev. Sol. State. Mater. Sci. 14 (1988) S1.
[27] B.J. Garrison, N. Winograd, D.E. Harrison, J. Chem. Phys. 69 (1978) 1440.
[28] M.S. Stave, D.E. Sanders, T.J. Raeker, A.E. DePristo, J. Chem. Phys. 93 (1990) 4413.
[29] T.J. Raeker, A.E. DePristo, Int. Rev. Phys. Chem. 10 (1991) 1.
[30] C.L. Kelchner, D.M. Halstead, L.S. Perkins, N.M. Wallace, A.E. DePristo, Surf. Sci. 310 (1994) 425.
[31] J. Tersoff, Phys. Rev. B 37 (1988) 6991.
[32] A. Wucher, B.J. Garrison, J. Chem. Phys. 105 (1996) 5999.
[33] P. Sigmund, in: R. Behrisch (Ed.), Sputtering by Particle Bombardment, vol. 1, Springer-Verlag, Berlin, 1981, p. 5.
[34] A. Delcorte, X. Vanden Eynde, P. Bertrand, D.F. Reich, Nucl. Instrum. Meth. B 157 (1999) 138.
[35] A. Delcorte, X. Vanden Eynde, P. Bertrand, D.F. Reich, Int. J. Mass Spectrom. 189 (1999) 133.